# Principle of ferroelectric domain imaging using atomic force microscope

Seungbum Hong[a] and Jungwon Woo
*Electronic and Optical Materials Laboratory, Korea Advanced Institute of Science and Technology, Taejon 305-701, Korea*

Hyunjung Shin and Jong Up Jeon
*Nano System Lab, Samsung Advanced Institute of Technology and Creative Research Initiatives, Suwon, Korea*

Y. Eugene Pak
*MEMS Lab, Samsung Advanced Institute of Technology, Suwon, Korea*

Enrico L. Colla and Nava Setter
*Ceramic laboratory, Swiss Federal Institute of Technology, Lausanne, Switzerland*

Eunah Kim and Kwangsoo No
*Electronic and Optical Materials Laboratory, Korea Advanced Institute of Science and Technology, Taejon 305-701, Korea*

(Received 10 February 2000; accepted for publication 19 October 2000)

The contrast mechanisms of domain imaging experiments assisted by atomic force microscope (AFM) have been investigated by model experiments on nonpiezoelectric (silicon oxide) and piezoelectric [$Pb(Zr,Ti)O_3$] thin films. The first step was to identify the electrostatic charge effects between the tip, the cantilever, and the sample surface. The second step was to explore the tip–sample piezoelectric force interaction. The static deflection of the cantilever was measured as a function of dc bias voltage ($V_{dc}$) applied to the bottom electrode (*n*-type Si wafers) for noncontact and contact modes. In addition, a small ac voltage ($V_{ac}\sin\omega t$) was applied to the tip to measure the amplitude ($A_\omega$) and phase ($\Phi_\omega$) of the first harmonic ($\omega$) signal as a function of $V_{dc}$. By changing from the noncontact to the contact mode, a repulsive contribution to the static deflection was found in addition to the attractive one and a 180° phase shift in $\Phi_\omega$ was observed. These results imply that in the contact mode the cantilever buckling is induced by the capacitive force between the cantilever and the sample surface. This interaction adds to the tip–sample piezoelectric interaction thereby overlapping the obtained tip vibration signal. Therefore, the antiparallel ferroelectric domain images obtained at zero dc bias voltage will show a variation in $A_\omega$ but a negligible one in $\Phi_\omega$. The capacitive force contribution to the tip vibration signal was further verified in piezoelectric hysteresis loop measurement assisted by the AFM. The observed vertical offset of the loops was explained by the contact potential difference between the cantilever and the bottom electrode. The shape of the curve could be explained by the capacitive force interaction combined with the tip–sample piezoelectric interaction. The experimental results obtained in this study support the interpretation of the cantilever–sample capacitive force contribution to the tip vibration signal in ferroelectric domain imaging experiments using AFM as a probing tool. The use of a large area top electrode between the tip and the sample resulted in the elimination of the electrostatic cantilever–sample interaction with negligible degradation of the domain contrast. This method proved to be successful because the cantilever–sample interaction was hardly detected and only the tip–sample interaction was observed.  [DOI: 10.1063/1.1331654]

## INTRODUCTION

It has been recently shown that the structure and dynamics of ferroelectric domains in thin films can be studied *in situ* by using an atomic force microscope (AFM). This technique enables the observation of the domain configuration in the projection planes of the films. The observation of the behavior of ferroelectric domains under variable external electric fields combined with conventional electrical measurements is very instructive for the understanding of polarization related processes in ferroelectric thin films.[1–4] Most of these studies are based on the AFM–tip/$Pb(Zr,Ti)O_3$ (PZT) film/bottom electrode (BE) configuration. A small ac voltage is applied between the AFM–tip and BE to induce a local piezoelectric vibration, which is generally believed to be detectable by the AFM tip. The amplitude of the vibration signal provides information on the magnitude of the piezoelectric coefficient, while the phase signal determines the polarization direction. Due to the absence of the top electrode (TE), one can observe the ferroelectric domains and the surface topography at the same time and easily correlate the microstructure and the domain polarization behavior.[3]

[a]Present address: Ceramic Laboratory, Swiss Federal Institute of Technology, Lausanne, Switzerland. Permanent address: Nano System Lab, Samsung Advanced Institute of Technology, Suwon, Korea.

 

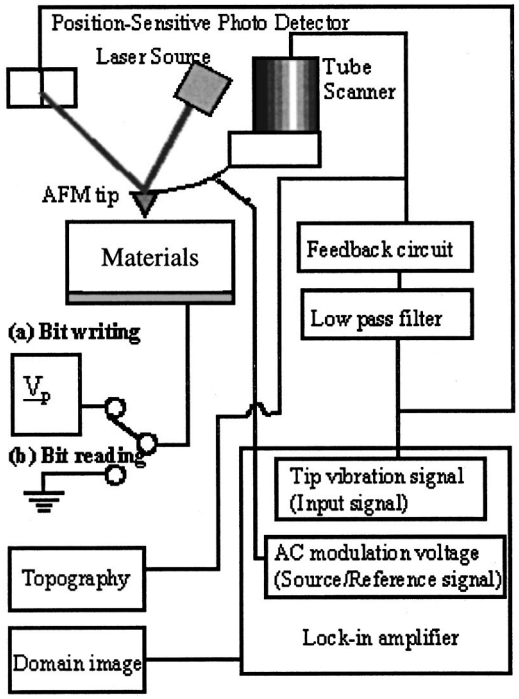


FIG. 1. The schematic diagram of an experimental setup. The system consists of AFM, lock-in amplifier, power supply, and PC.

However, a few questions relevant to the origin and interpretation of the domain contrast remain unanswered. As mentioned above, the origin of the domain contrast obtained by this method is expected to be the piezoelectric deformation. However, recently proposed was a different mechanism where the surface electric charge effect is the dominant contributing factor to the domain contrast observed in thin films.[5] The ferroelectric domain imaging in the contact mode was renamed ''dynamic contact mode electrostatic force microscopy (DC-EFM)'' instead of piezoelectric force microscopy (PFM).[5] The force–distance and tip–vibration amplitude-distance curves were measured simultaneously on a triglycine sulfate (TGS) ferroelectric sample.[5] From those curves, it was found that there exists a sustained vibration of 1 nm when in the contact mode. To explain this vibration the existence of an air gap between the tip and the sample surface was suggested. The surface charge density was calculated based on the assumption of an air gap of 1 nm, which was in good agreement with the measured value by electrical characterization. It was also argued that the calculated piezoelectric displacement for their sample was about ~0.01 nm far below the measured sustained vibration. Finally, the temperature dependence of the domain contrast was contradictory to the expected trend of the piezoelectric coefficient. Therefore, the electrostatic force interaction between the tip and sample was considered to be the major contributing factor to the domain contrast.

However, the reported existence of the large sustained vibration induced by the attractive capacitive force is incompatible with the steep repulsive atomic force that the tip experiences. This intriguing inconsistency represents the starting point of the present work where the origin of the sustained vibration is explored. The electrostatic force effect between a tip and a sample surface was first investigated on *n*-type Si wafers covered with native oxide and thermal oxide, which show a negligible piezoelectric effect. PZT thin films were also studied by the same technique to explore the piezoelectric contribution to the ferroelectric domain imaging using AFM.

In this study, it is attempted to separate the different possible contributions to the domain contrast mainly considering the tip–sample and cantilever–sample interactions. Based on the suggested model of the contrast mechanism, a few methods to suppress the cantilever–sample interaction in order to obtain the pure tip–sample interaction are suggested.

## EXPERIMENTAL PROCEDURE

A commercial atomic force microscope (AFM, Park Scientific Instruments, Autoprobe M5) connected to a lock-in amplifier (SR830, Stanford Research Systems) was used, as shown in Fig. 1. The AFM tips (PSI, UL06A) are made of boron doped *p*-type Si, and their height and radius are about 3 $\mu$m and 20 nm, respectively, estimated from scanning electron microscope (SEM) images. The length, width, and thickness of the cantilever are 180, 25, and 1.0 $\mu$m, respectively. The force constant and the resonance frequency of the cantilever are 0.26 N/m and 40 kHz, respectively. The samples were *n*-type Si wafers with [100] orientation covered with native oxide (sample $\alpha$) and 500 nm thick thermally grown $SiO_2$ (sample $\beta$), 270 nm thick $Pb(Zr_{0.4}Ti_{0.6})O_3$ film (sample $\gamma$) on $Pt/TiO_2/SiO_2/Si$, and 909 nm thick $Pb(Zr_{0.45}Ti_{0.55})O_3$ film (sample $\theta$) on $Pt/TiO_2/SiO_2/Si$. During the experiment, ac voltage of 1 $V_{pp}$ (peak to peak) at 17 kHz was applied to the AFM tip while dc bias voltages or bipolar single pulses with sinusoidal shape were applied to the bottom electrode. For all the experiments, the AFM tip was maintained at a fixed $X-Y$ position so that all the data were acquired from one position on the sample. For the noncontact mode, the tip to sample distance was 3.3 $\mu$m. This distance was kept constant by disabling the feedback loop for the *Z* piezotube scanner. However, *z* drifts of 40–50 nm were observed during the measurement, resulting in the position uncertainty of about 1.5% at this distance.

First, the tip deflection was imaged for both cases, contact and noncontact modes in sample $\alpha$. The time evolution of the tip vibration signal was collected at intervals of 0.2 s in order to fit the acquisition features of the instrument. The tip vibration signals collected at each period were assembled to visualize the cantilever movement. An ac voltage of 1 $V_{pp}$ at 17 kHz was applied to the tip while sinusoidal shaped pulses with an amplitude of 20 $V_{pp}$ and a period of 0.05 s (20 Hz) were applied to the sample at intervals of 0.2 s. The static deflection and the first harmonic ($\omega$) signal of the induced tip vibration were recorded simultaneously. The first harmonic signal (amplitude $A_\omega$ and phase $\Phi_\omega$) was investigated by varying $V_{dc}$ on the Si wafers in samples $\alpha$ and $\beta$. The tip to sample distances in the noncontact mode were 3337 nm±55 nm and 3431 nm±38 nm for samples $\alpha$ and $\beta$, respectively. The last experiment was repeated on sample $\gamma$.

Piezoelectric hysteresis loop measurements were conducted on samples $\gamma$ and $\theta$ using the AFM. Both continuous

dc and pulse dc modes were used. The former mode consists of applying voltage while measuring the piezoelectric signal, whereas the latter mode consists of applying a pulse voltage and measuring the piezoelectric signal at zero dc bias voltage. The voltage was varied between −10 and 10 V for sample $\gamma$ and between −15 and 15 V for sample $\theta$.

## RESULTS AND DISCUSSION

Figure 2 shows the images of the static deflection, $A_{\omega 1}$ and $\Phi_{\omega 1}$ for both noncontact [Figs. 2(a)–2(c)] and contact [Figs. 2(d)–2(f)] modes. The voltage profile applied to the bottom electrode (sine pulse) is shown under each image to easily correlate the perturbation with the measured signal. If one assumes that the displacement of the tip–cantilever is a linear function of the external force, the static deflection, and the tip vibration signal at $\omega_1$ frequency can be expressed as follows:

$$z_{\text{static}} = \frac{F_{\text{static}}}{k_{\text{lever}}} = \frac{\Gamma}{k_{\text{lever}}}\left(\frac{V_1^2}{2} + (V_c - V_{\text{dc}})^2\right), \tag{1}$$

$$z_{\omega_1} = \frac{2\Gamma}{k_{\text{lever}}}(V_c - V_{\text{dc}})V_1 \sin\omega_1 t = A_{\omega_1}\cos\Phi_{\omega_1}\sin\omega_1 t,$$

$$A_{\omega_1} = \left|\frac{2\Gamma}{k_{\text{lever}}}(V_c - V_{\text{dc}})V_1\right|, \tag{2}$$

$$\Phi_{\omega_1} = \begin{cases} 0, & \text{if } V_{\text{dc}} > V_c, \\ 180, & \text{if } V_{\text{dc}} < V_c, \end{cases}$$

where $\Gamma$ is $(1/2)(\partial C/\partial z)$, $C$ is the electric capacitance between the tip–cantilever system and the Si wafer, $k_{\text{lever}}$, is the spring constant of the cantilever, $V_c$ is the contact potential difference (CPD) between the Si wafer and the tip–cantilever system, $V_{\text{dc}}$ is the voltage profile applied to the Si wafer (dc or sine pulse), and $V_1 \sin\omega_1 t$ is the ac voltage applied to the tip. According to Eqs. (1) and (2), the static deflection is always attractive, $A_{\omega 1}$ is proportional to the absolute value of the difference between applied voltage and CPD, and $\Phi_{\omega 1}$ changes its value from 0° to 180° when, on decreasing $V_{\text{dc}}$, one obtains $V_{\text{dc}} < V_c$.

For the noncontact regime, the static deflection shows an attractive interaction under nonzero voltage. The asymmetric tip deflection can be explained by the CPD between the *n*-type Si wafer and the *p* type Si tip. Knowing the resistivity (1.2–2 Ω cm)[6] of the *n*-type Si wafer, one can estimate the dopant concentration to be $10^{15}$–$10^{16}/\text{cm}^3$. The boron doped tip is assumed to have an acceptor concentration of $10^{17}$–$10^{19}/\text{cm}^3$. The estimated work function difference $(\phi_{\text{tip}} - \phi_{\text{bottom}})$ between the tip–cantilever system and the *n*-type Si wafer (as the bottom electrode) is −0.7 to −0.8 eV. If $V_c$ arises only from the work function difference, $V_c$ is expected to be −0.7 to −0.8 V. If we assign the value −0.7 V to $V_c$ and all the other known values to the parameters in Eq. (1), the net displacement, $z_{\text{pulse}} - z_{\text{background}}$, can be calculated and plotted as a function of time (Fig. 3). The calculated profile shows a good agreement with the experimental result for the noncontact mode [Fig. 2(a)]. The amplitude and phase of the tip $\omega_1$–vibration signal are also in good agreement with Eq. (1) for the noncontact mode.

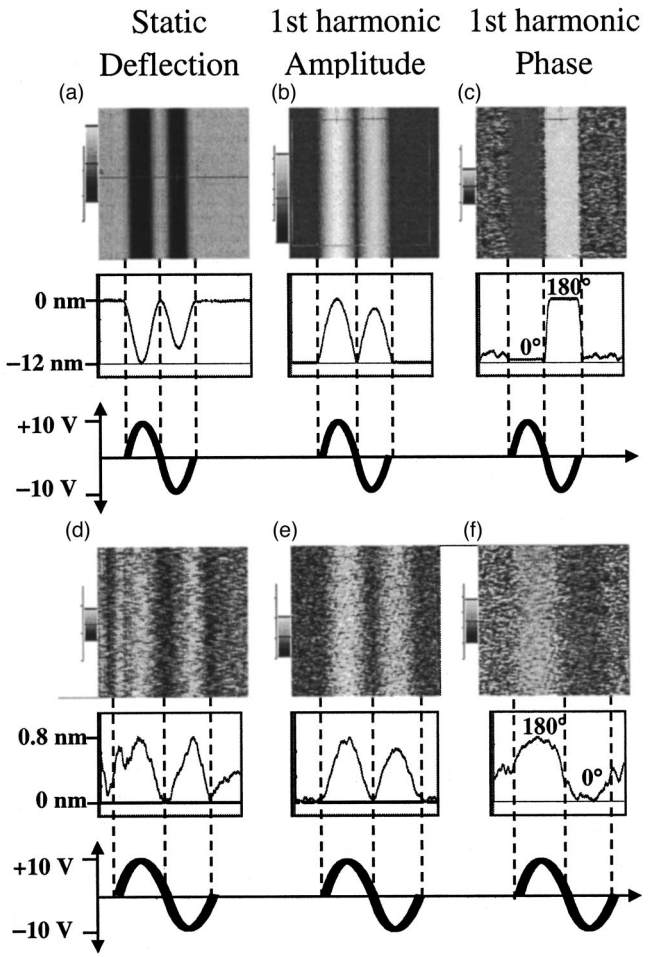


FIG. 2. The static deflection of the tip–cantilever system [(a) and (d)], the amplitude [(b) and (e)] and phase [(c) and (f)] of the tip vibration signal at $\omega_1$ frequency for noncontact [(a)–(c)] and contact [(d)–(f)] modes.

On the other hand, for the contact mode, the net displacement of the static deflection shows a large portion of white contrast (repulsive movement) along with a small portion of black contrast (attractive movement). The phase of the tip $\omega_1$–vibration shows a reversed trend compared with the noncontact mode [Figs. 2(d)–(z)]. These results cannot

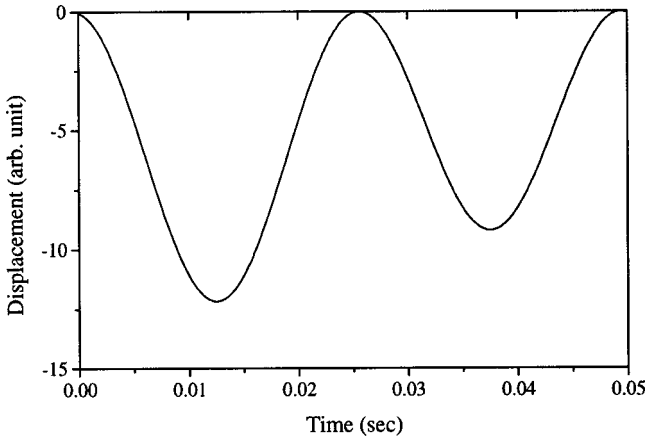


FIG. 3. The calculated profile of displacement when a sinusoidal voltage profile is applied to the tip.

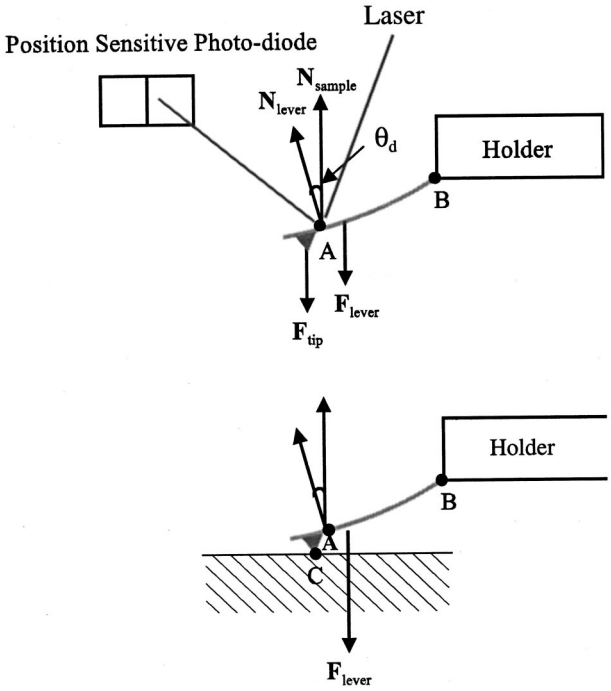


FIG. 4. The schematic diagram of the tip–cantilever system. Point A is the position where the laser beam bounces off, point B is the pivot that cantilever rotates around, and point C is the contact point between the tip and the sample surface. $\mathbf{F}_{tip}$ and $\mathbf{F}_{lever}$ are the forces acting on the tip and the cantilever, respectively. $\mathbf{N}_{lever}$ and $\mathbf{N}_{sample}$ are the surface normal vectors of the cantilever and the sample, respectively. $\theta_d$ is the angle between $\mathbf{N}_{lever}$ and $\mathbf{N}_{sample}$, and is measured by the position sensitive photodiode (PSPD).

be due to the capacitive force between the tip and the sample surface, as was recently explained.[5] If the capacitive force between the tip and the sample surface was determining the EFM signal, the only expected change would be the decrease in both the magnitude of the attractive displacement and the amplitude of the tip $\omega_1$-vibration signal.

The observed trends in the static tip deflection and the tip vibration signal at $\omega_1$ frequency can be explained in a different way. As shown in Fig. 4, the tip–cantilever system rotates around the pivot B in the noncontact mode. Therefore, $\mathbf{F}_{tot}$ on the tip–cantilever system increases $\theta_d$ (Fig. 4). As a result, the laser beam spot on the position sensitive photodiode (PSPD) moves to the left direction and it is recorded as an attractive displacement. However, in the contact mode, the tip experiences a steep increase in the repulsive atomic force as the distance decreases.[7] Accordingly, $\mathbf{F}_{tip}$ has little effect on the tip movement. The tip becomes nearly fixed in the $z$ direction and acts as another pivot (Fig. 4 point C). In the contact mode, only the cantilever is relatively free to move, so the major contributing factor to the deflection of the tip–cantilever system is $\mathbf{F}_{lever}$. Since point A is closer to point C than B, $\mathbf{F}_{lever}$ will decrease $\theta_d$. Therefore, the beam spot moves to the right direction and it is recorded as a repulsive displacement. This means that $\Gamma$ becomes a positive constant, $\Gamma'(\cong -\Gamma_{lever})$ for the contact mode in our measurement set-up. Therefore, Eq. (2) should be modified as follows:

$$z_{\omega_1} = \frac{2K\Gamma'}{k_{lever}}(V_c - V_{dc})V_1 \sin \omega_1 t,$$

$$A_{\omega_1} = \left|\frac{2K\Gamma'}{k_{lever}}(V_c - V_{dc})V_1\right|, \tag{3}$$

$$\Phi_{\omega_1} = \begin{cases} 180, & \text{if } V_{dc} > V_c, \\ 0, & \text{if } V_{dc} < V_c, \end{cases}$$

where $K$ is a positive calibration constant smaller than unity. This reduction factor comes from the fact that the cantilever movement is restricted by the two pivots B and C. It should be noted that $V_c$ nearly equals $V_{c,lever}$ since $\mathbf{F}_{lever}$ mainly contributes to the deflection of the tip-cantilever system.

In Eq. (3) the tip vibration induced by tip–sample capacitive force ($\mathbf{F}_{tip}$) was not taken into account. Its displacement induced by $\mathbf{F}_{tip}$ is expected to be very small due to the steep increase in the atomic force as the tip–sample distance decreases. In the noncontact mode, $\mathbf{F}_{tip}$ should balance only the restoring force of the cantilever, which is a linear function of the displacement. In the contact mode, $\mathbf{F}_{tip}$ should balance the atomic force and the restoring force of the cantilever. However, the repulsive atomic force is orders of magnitude larger than the restoring force of the cantilever, and can be ignored. Therefore, the tip displacement plays a minor role in the deflection of the tip–cantilever system and the trend of the observed sustained vibration should be the same as that when only $\mathbf{F}_{lever}$ is responsible for its deflection.

The interpretation expressed by Eq. (3) explains the trends of repulsive displacement of the tip deflection [Fig. 2(d)], the decrease in $A_{\omega 1}$ [Fig. 2(e)] and the change of $\Phi_{\omega 1}$ from 180° to 0° [Fig. 2(f)] at the bottom electrode voltage transition from +10 V to −10 V. However, it cannot explain the attractive displacement (i.e., dark contrast) in the static deflection. When the cantilever is in contact with the sample, any normal force acting on the cantilever can also lead to a longitudinal motion. Because of the normal force acting on the tip–cantilever system, the tip can perform a stick-slip motion along the surface, which can, in turn, lead to a normal deflection signal due to the buckling of the cantilever. This effect will occur simultaneously to the buckling of the cantilever due to the electrostatic force between the lever and the bottom electrode. The occurrence of both black and white contrast in the contact deflection signal is considered to arise from the interference of the longitudinal motion of the tip.

In the second experiment the dependencies of $A_{\omega 1}$ and $\Phi_{\omega 1}$ on $V_{dc}$ (Figs. 5 and 6) are investigated. In the noncontact mode, as $V_{dc}$ increases up to $V_c$, the amplitude decreases linearly, and the phase remains 180°. For $V_{dc} > V_c$, as $V_{dc}$ increases, the amplitude increases linearly, and the phase changes to 0°. This is well explained by Eq. (2). In the contact mode, the amplitude shows the same trend. Only the slope of the amplitude versus $V_{dc}$ curve decreases in the contact mode. However, the phase is 0° and 180° for $V_{dc} < V_c$ and $V_{dc} > V_c$, respectively. This is a reversed trend compared with the noncontact mode and can be explained by Eq. (3). The above trends support the validity of our model (Fig. 4).

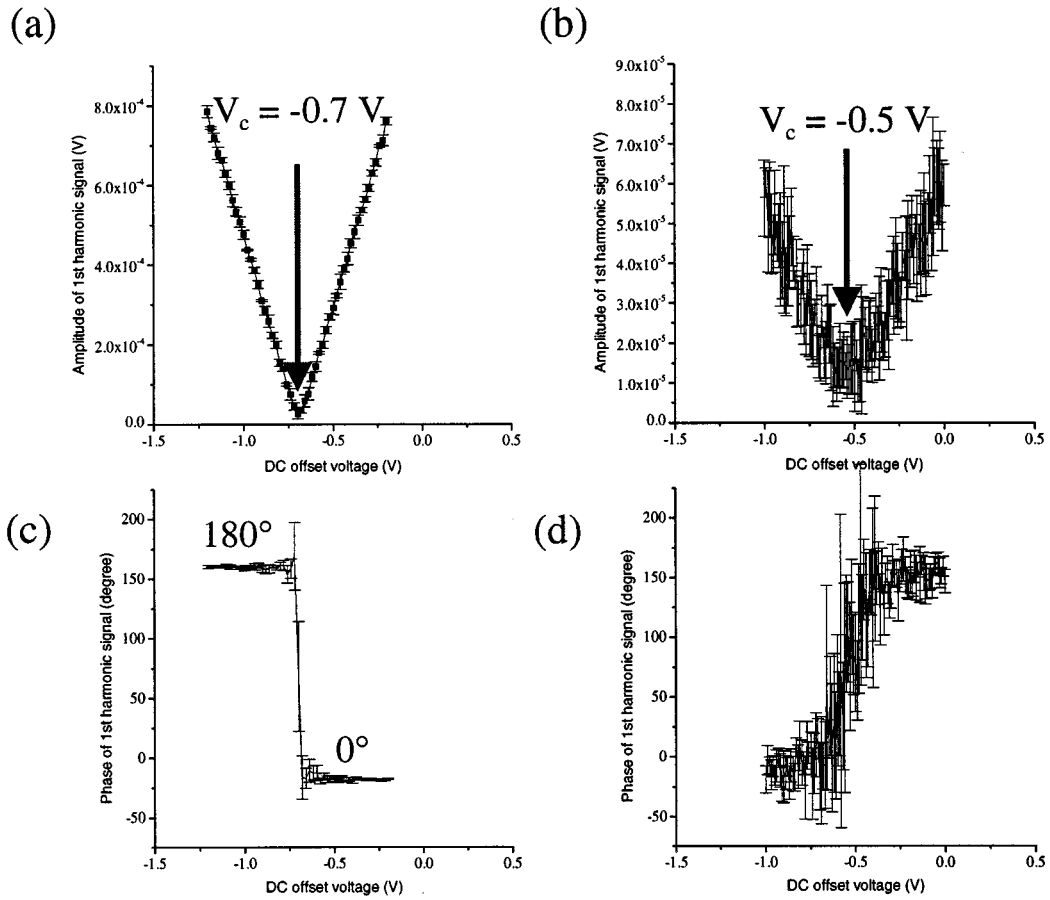


FIG. 5. The amplitude [(a) and (b)] and phase [(c) and (d)] of the first harmonic signal of the tip–cantilever deflection in both noncontact [(a) and (c)] and contact [(b) and (d)] modes. The sample is an *n*-type Si wafer covered with a native oxide (sample $\alpha$).

The results of both experiments show that $\mathbf{F}_{\text{lever}}$ is the governing factor for the DC-EFM signal on $SiO_x/Si$ samples. They also show that the tip is virtually fixed in the *z* direction by the steep increase of the repulsive atomic force as a function of distance. However, it should be noted that the tip might not be fixed in the longitudinal direction, as discussed above.

The clarification of the major effect of $\mathbf{F}_{\text{lever}}$ on the DC-EFM signal provides improved insight into the interpretation of the domain imaging in ferroelectric materials or the trapped charge imaging in insulators. The effect of $\mathbf{F}_{\text{lever}}$ on the domain images can be expressed by an offset to $A_{\omega 1}\cos(\Phi_{\omega 1})$. The mapping of the domains with opposite polarization obtained by contact mode AFM is correct only if the $\mathbf{F}_{\text{lever}}$ effect is the same for the entire region. This corresponds to the case where the domain size is very small compared to the effective size of the cantilever plate and the distribution of the opposite domains is homogeneous. Even in this case, due to the existence of $\mathbf{F}_{\text{lever}}$, the phase difference between the two opposite domains in ferroelectric thin films can be much less than 180°s.

From the above analysis, one can easily see that the evidences suggested[5] for an electrostatic force contribution to the tip vibration signal are, in fact, the indication for an electrostatic force contribution between the cantilever and the sample. The capacitive force acting on the tip induces negligible displacement because the atomic force steeply increases for very small displacements. Therefore, it is suggested that the tip vibration signal in ferroelectric materials consists of the piezoelectricity of the film and the electrostatic force interaction between the cantilever and the bottom electrode. In the following section the results obtained with the PZT sample are presented and discussed.

Figure 7 shows the first harmonic amplitude and phase of the tip vibration signal in the noncontact mode. The tip to sample distance is 3 $\mu$m. Since the Pt bottom electrode has a higher work function (5.3–5.6 eV) than the tip does (4.9–5.0 eV), it is found that $V_c \approx 0.3-0.7$ V. Taking the distance dependence of $V_c$ into account, one can find that our experimental result of $V_c = 0.45$ V agrees fairly well with the estimation. The amplitude curve shows a clear V shape that is a characteristic of Kelvin probe microscopy and is in accordance with Eq. (2). The phase shows a transition from 180° to 360° or 0° as expected from Eq. (2).

In the contact mode, the first harmonic amplitude and phase signals were measured for domains of both orientations, top to bottom and bottom to top. As can be seen in Fig. 8, the phase signal shows a reversed trend when compared with the noncontact mode, irrespective of domain orientation. This clearly shows that the cantilever–sample capacitive force contribution to the piezoresponse signal still takes the major portion. However, piezoelectricity distinguishes the direction of the domains and this effect moves the position of $V_c$ from 0.66 V to 0.61 V when we change the po-

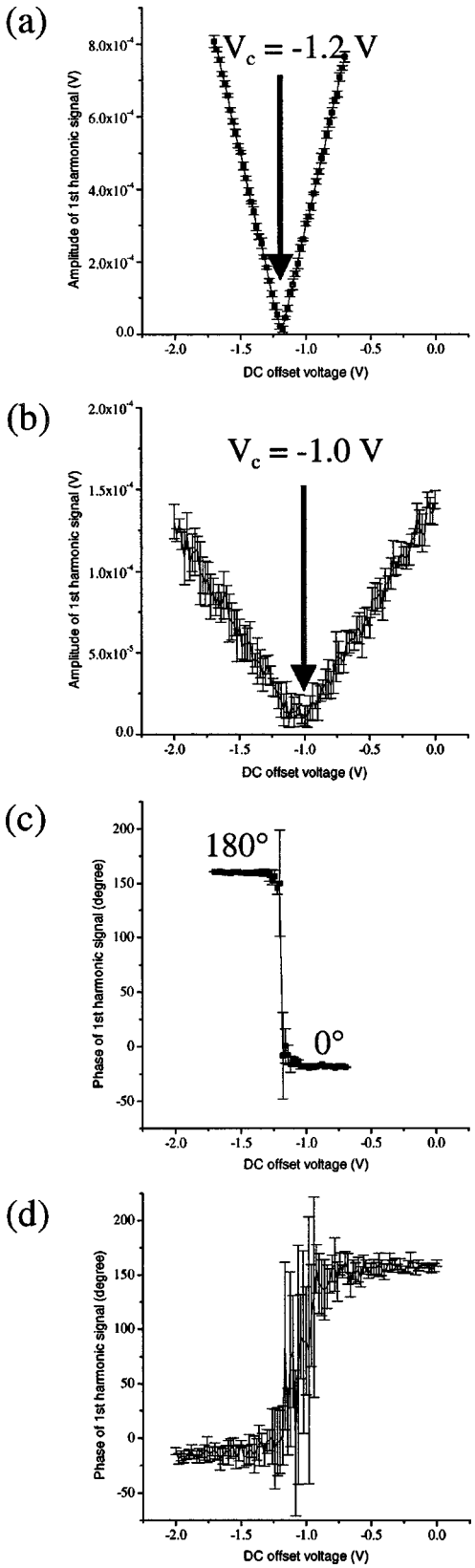


FIG. 6. The amplitude [(a) and (b)] and phase [(c) and (d)] of the first harmonic signal of the tip–cantilever deflection in both noncontact [(a) and (c)] and contact [(b) and (d)] modes. The sample is an *n*-type Si wafer covered with a thermally grown oxide of 500 nm thickness (sample $\beta$).

larization state from the $\downarrow$ to the $\uparrow$ state, as shown in Fig. 8. Note that this apparent $V_c$ shift is not coming from the electrical effect but from the mechanical effect. Since only ac

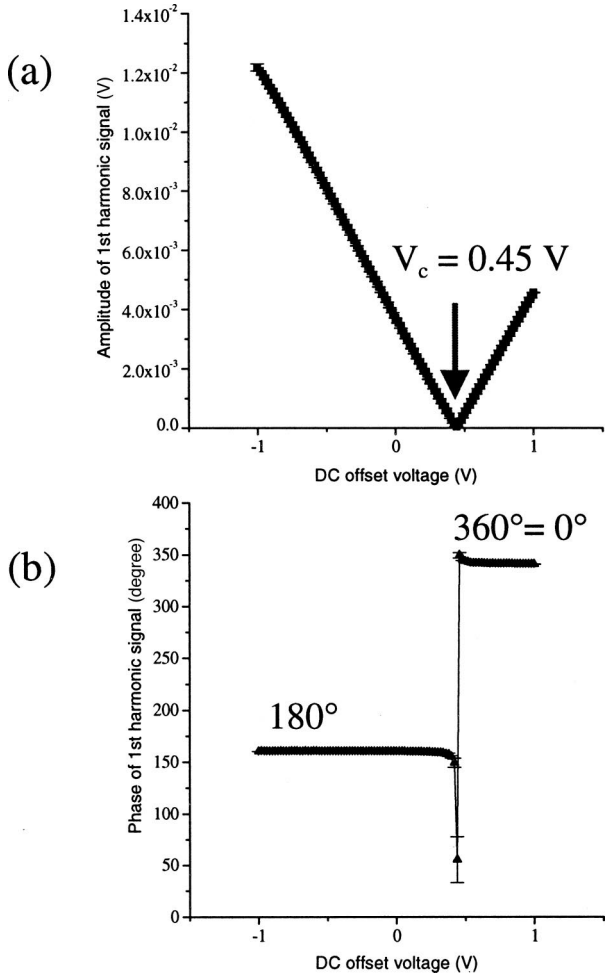


FIG. 7. The amplitude (a) and phase (b) of the first harmonic signal of the tip–cantilever deflection in the noncontact mode for sample $\gamma$.

voltage is applied to the system without a dc bias field in domain imaging, the piezoresponse signal for opposite domains corresponds to the points where $V_{dc}=0$ in Fig. 8. It is found that there will be no or only a slight phase change for opposite domains for the AFM–tip/PZT/Pt system. Moreover, due to the apparent $V_c$ shift in voltage axis, the amplitude will decrease when changing the domain direction from $\downarrow$ to $\uparrow$.

Figure 9 shows the relationship between the piezoresponse versus $V_{dc}$ and the relevant domain images of bits written in an antiparallel matrix. We imaged in both left to right and right to left directions to see if there is a friction force dependence of the domain images, as reported by Luthi *et al.*[8] As seen in Fig. 9 there was no essential difference between the two scan directions. In Fig. 9 it is found that the phase images do not show a significant change for antiparallel domains written as bits, whereas the amplitude images show protruding bits as expected from the piezoresponse versus the $V_{dc}$ curve.

The principle of domain imaging can be summarized as follows: the domain contrast consists of the piezoelectric interaction between the tip and the sample and the electrostatic force interaction between the cantilever and the bottom electrode. This principle can be better illustrated by analyz-

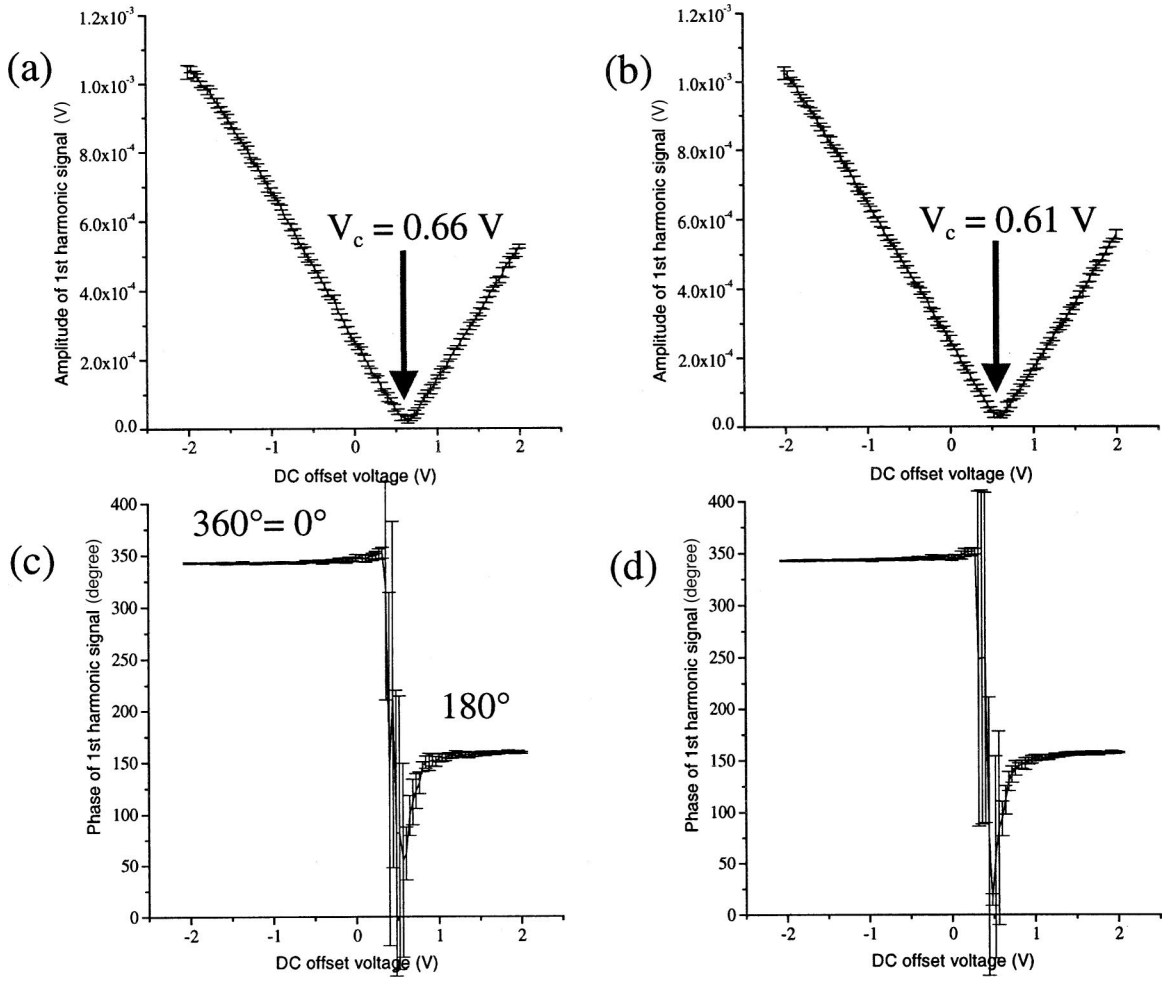


FIG. 8. The amplitude [(a) and (b)] and phase [(c) and (d)] of the first harmonic signal of the tip–cantilever deflection in the contact mode for negatively [top to bottom, (a) and (c)] and positively [bottom to top, (b) and (d)] poled domains (sample $\gamma$).

ing the piezoresponse hysteresis loop measured by AFM in the continuous dc and the pulse dc mode. Most of the $P(E)$ hysteresis or strain versus $V_{dc}$ curves are measured in the continuous dc mode. It consists of measuring the induced piezoelectric vibration under continuously increasing and decreasing the additional dc voltage [Fig. 10(a)]. However, this approach was rarely used for an AFM analysis of domain structures. The one that was generally used is depicted in Fig. 10(b). It operates as follows: the desired dc voltage is applied for a determined period of time and subsequently released to measure the piezoelectric signal at zero dc. With this configuration the cantilever–sample capacitive force is expected to be constant. Therefore the obtained signal information must be governed by the tip–sample interaction only. It has to be pointed out that the measured polarization evolution will not be exactly the same for the two approaches. For instance the ''polarization back-switching'' effects and opposite domain growth after nucleation will both behave in a very different way. As a consequence the coercive field obtained with the pulsed mode is clearly expected to be larger than with the continuous mode. Within the frame of the proposed model where the collected signal is determined by both, the piezoelectric force interaction between the tip and the sample and the electrostatic force interaction between the cantilever and the sample, $A_{\omega 1}\cos\Phi_{\omega 1}$ can be described by the following equations:

$$A_{\omega 1}\cos\Phi_{\omega 1}=\begin{cases}-\dfrac{2K\Gamma_{\text{lever}}}{k_{\text{lever}}}(V_{\text{dc}}+V_c)V_{\text{ac}}+d_{33}V_{\text{ac}}, \\ \qquad \text{for the } \downarrow \text{ domain}, \\ -\dfrac{2K\Gamma_{\text{lever}}}{k_{\text{lever}}}(V_{\text{dc}}+V_c)V_{\text{ac}}-d_{33}V_{\text{ac}}, \\ \qquad \text{for the } \uparrow \text{ domain}.\end{cases} \tag{4}$$

The first term of each of the right sides of Eq. (4) is the capacitive contribution of the cantilever, whereas the second term is the piezoelectric contribution. The sign of $V_{dc}$, was changed because in this case $V_{dc}$ is applied to the tip [Eq. (4)] compared to the cases of Eqs. (2) and (3) for which the dc bias voltage was applied to the bottom electrode. This change enables us to plot the obtained results in the standard ferroelectric loop style. By using Eq. (4), one can calculate the tip vibration signal as a function of $V_{dc}$ for both configurations [Figs. 11(a) and 11(b)]. An interesting result is that the vertical shift of the hysteresis loop arises from the contact

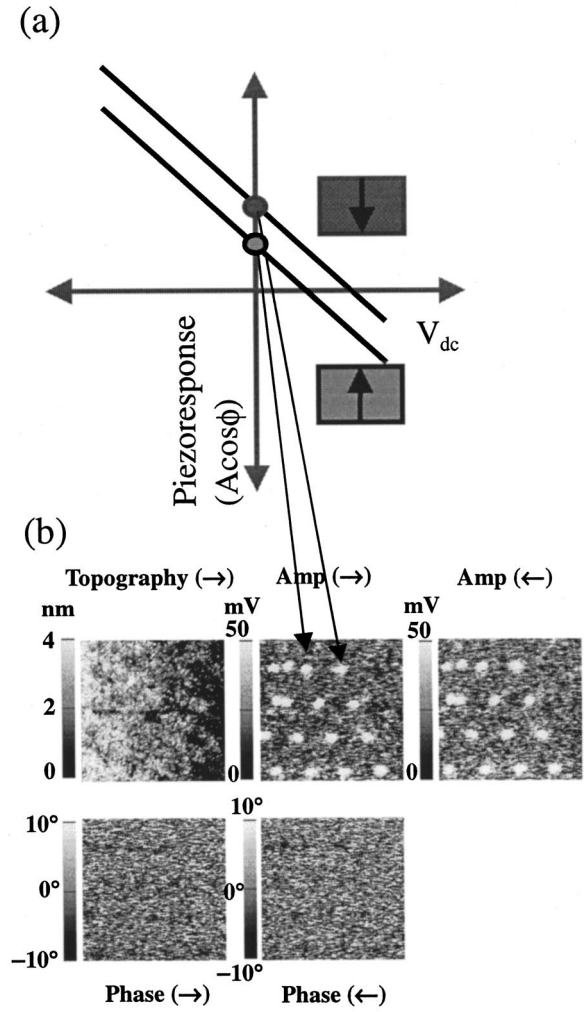


FIG. 9. (a) Piezoresponse curve of negative (↓) and positive (↑) domains as a function of $V_{dc}$ to the bottom electrode. (b) Bit arrays of negative domains embedded in a matrix of positive domains. The pulse voltage and width were −18 V and 33 ms, respectively. (sample $\gamma$)

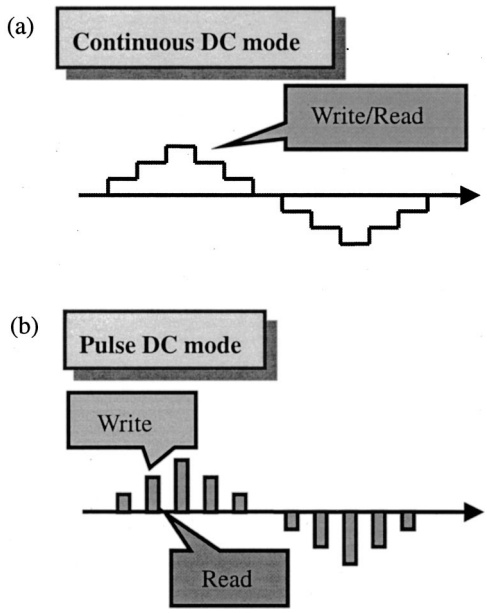


FIG. 10. The schematic diagram of (a) continuous dc and (b) pulse dc modes.

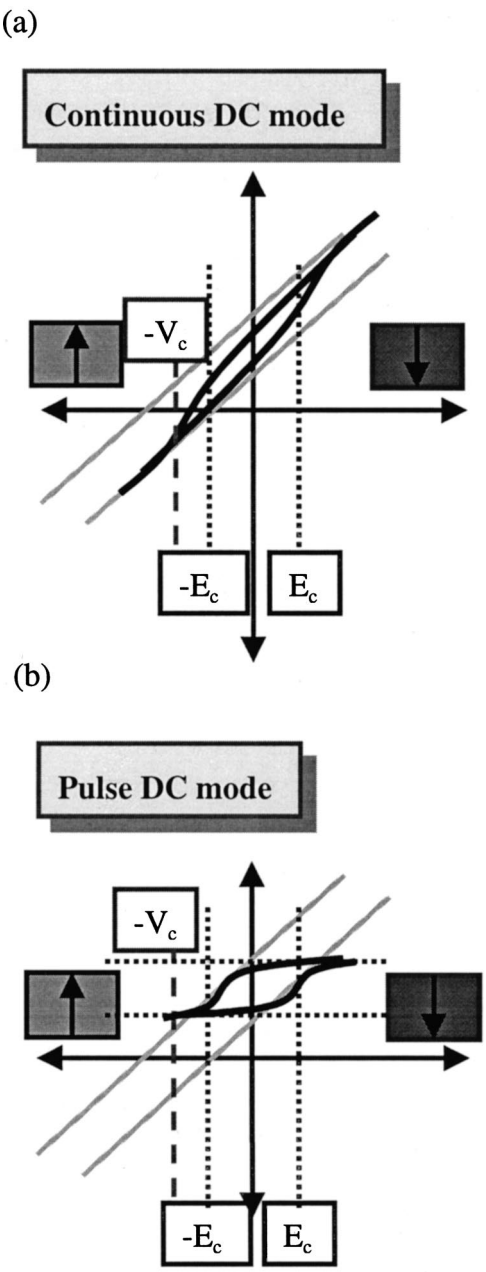


FIG. 11. The expected piezoresponse hysteresis loops in (a) continuous dc and (b) pulse dc modes.

potential difference between the tip–cantilever system and the bottom electrode. With $V_c > 0$ the vertical shift occurs upward and vice versa.

Figures 12(a) and 12(b) show the piezoresponse hysteresis curves of a $Pb(Zr_{0.4}Ti_{0.6})O_3$ thin film of thickness 270 nm (sample $\gamma$), obtained with the continuous and pulse dc mode, respectively. Both loop shapes are very similar to the calculated ones (Fig. 11) and the vertical shift is positive for both modes as predicted by Eq. (4) with $V_c = 0.7$ V.

Figures 13(a) and 13(b) show the similar piezoresponse hysteresis loops measured by other authors in the pulse dc mode.[3,9] It is surprising to see that for the virgin state the vertical shift of the loop is in accordance with our model. The virgin state of Fig. 13(a) shows a vertical shift upward whereas that of Fig. 13(b) does a negligible shift. This can be

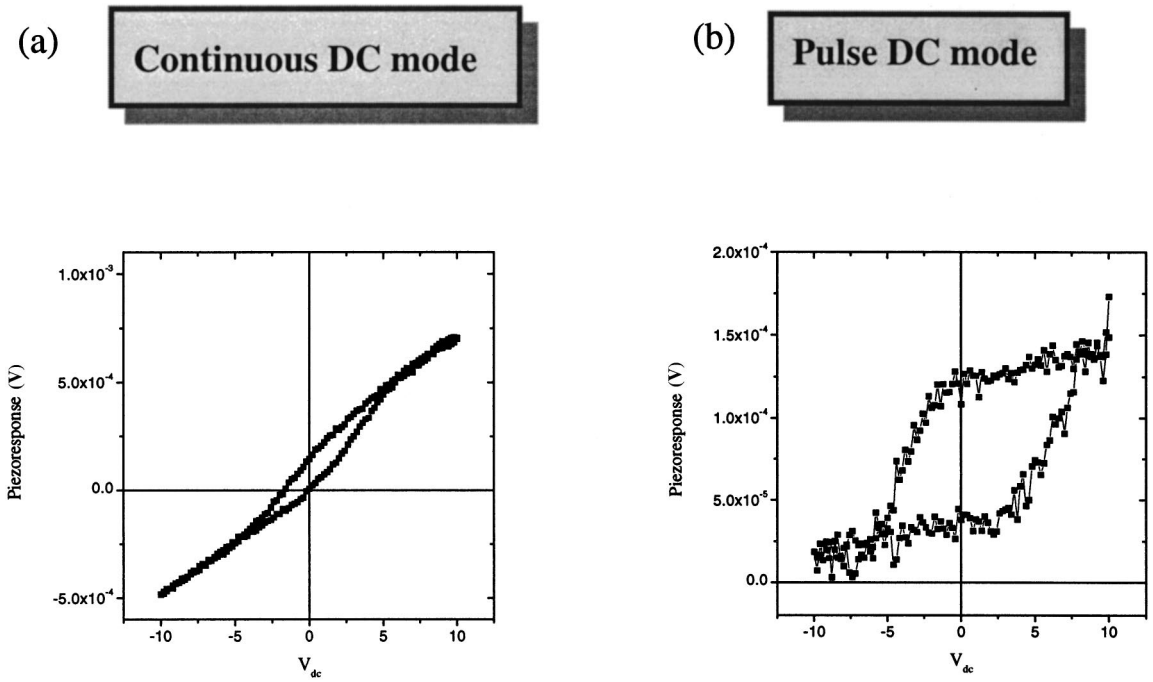


FIG. 12. Piezoresponse hysteresis loops of (a) continuous dc and (b) pulse dc modes for sample $\gamma$. The pulse width is 200 ms for the pulse dc mode. Note that $V_c = 0.7$ V, so a positive vertical shift occurs in the loops.

explained by CPD of +1.1 and 0 V, respectively, between the tip–cantilever system and the bottom electrode. It is worth noting that the relative vertical shift of the curve when comparing the virgin and the fatigued states of PZT in Fig. 13(a) can be attributed to the domain configuration, as explained by Gruverman *et al.*[3] The vertical shift of the curve for the virgin sample when using a different tip is coming from the contact potential difference between the tip–cantilever system and the bottom electrode.

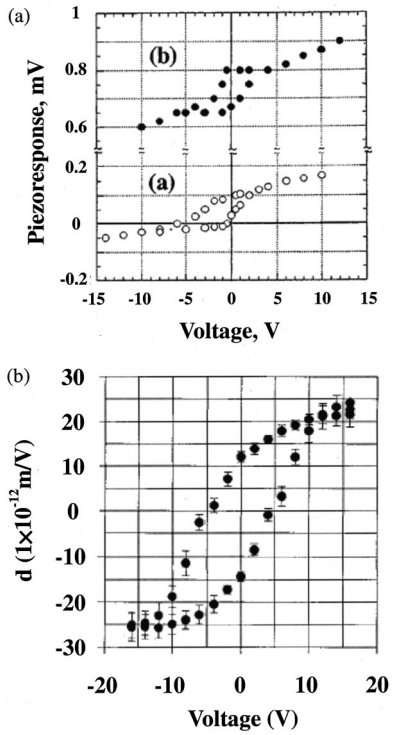


FIG. 13. Piezoresponse hysteresis loops for 180 nm thick $Pb(Zr_{0.53}Ti_{0.47})O_3$ film of virgin and fatigued ($6\times10^3$ switching pulses) with a $Si_3N_4$ tip coated by a Au and Pt bottom electrode. $V_c = 1.1$ V (CPD) between Pt and Au. (b) Piezoresponse hysteresis loops for 300 nm thick $Pb(Zr_{0.52}Ti_{0.48})O_3$ film with a Si tip coated by the Pt and Pt bottom electrode. $V_c = 0$ V (CPD between Pt and Pt). (See Refs. 3 and 9.)

Additional evidence supporting our interpretation is shown in Figs. 14(a) and 14(b). The sample used is a 909 nm $Pb(Zr_{0.45}Ti_{0.55})O_3$ thin film. Between the tip and the ferroelectric material there is a top electrode that is kept at the same potential as the tip and that is expected to screen the capacitive interaction of the cantilever with the bottom electrode. One can clearly see that the linear response [Fig. 14(b)] obtained with the continuous dc mode and without a top electrode becomes a well-defined piezoelectric hysteresis loop with the electrode screening effect [Fig. 14(a)]. The measured coercive field (continuous dc mode and screening electrode) is much closer to that obtained from the $P(E)$ hysteresis curve than that measured by the pulsed dc mode.

The above mentioned method minimizes the cantilever–sample capacitive contribution to the tip vibration signal in the contact mode, as previously demonstrated by Colla *et al.*[10] and Hong *et al.*[11] in ferroelectric fatigue and switching studies. Another effective way of suppressing the cantilever–sample interaction has been recently proposed by Hong *et al.*,[12] which suggests the use of a high aspect ratio tip with a stiffer cantilever. The results obtained using this method show a clear 180° phase shift for antiparallel ferroelectric domains.[12]

## CONCLUSION

The effect of the cantilever–sample capacitive force on the ferroelectric domain imaging in contact-mode AFM stud-

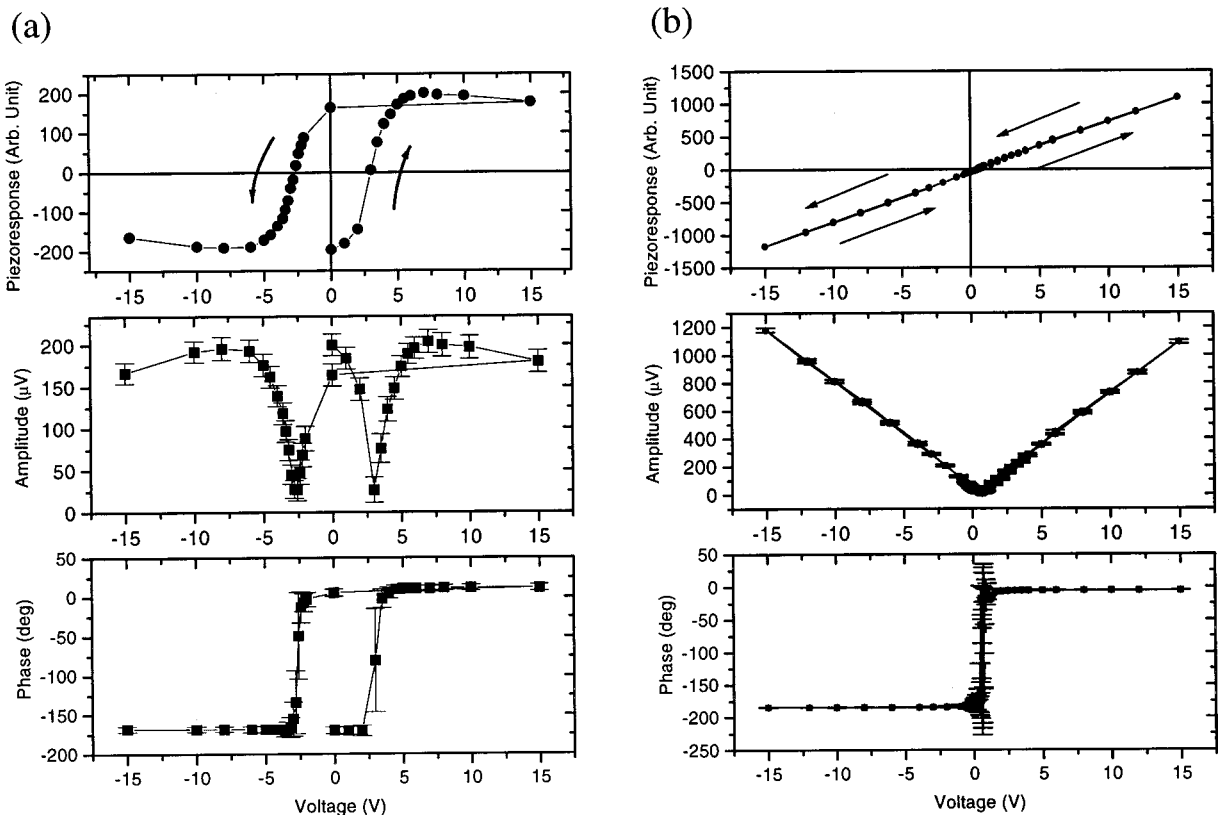


FIG. 14. Piezoresponse ($A\cos\phi$), amplitude (A), and phase ($\phi$) of the first harmonic signal as a function of $V_{dc}$ to the bottom electrode while 1 $V_{pp}$ ac voltage of 28.1 kHz is applied to the bottom electrode (a) with and (b) without a large area top electrode between the AFM tip and the sample surface (sample $\theta$).

ies was investigated and clarified. It was shown that the collected ac signal consists of the overlap of the tip vibration induced by the piezoelectric displacement and the undesired cantilever buckling induced by the capacitive force interaction. This explains the unexpected features of the piezoelectric hysteresis loops measured by AFM in continuous and pulse dc modes. Since the signal amplitude due to the capacitive interaction can be much larger than the piezoelectrically induced one, the information on the domain orientation is not always accessible. In order to suppress this interaction, the use of a high aspect ratio tip or specific screening electrodes were considered and preliminary results are very encouraging.

## ACKNOWLEDGMENTS

The authors gratefully acknowledge the primary financial support from Samsung Electronics, Inc. Additional supports from the Korean Ministry of Science and Technology through the Creative Research Initiative Program is gratefully acknowledged. One of our authors, S. Hong, gratefully acknowledges the financial support from the Korea Research Foundation through a Rising Researcher Fellowship.

[1] C. H. Ahn, T. Tybell, L. Antognazza, K. Char, R. H. Hammond, M. R. Beasley, O. Fischer, and J.-M. Triscone, Science **276**, 1100 (1997).
[2] K. Franke, Ferroelectr. Lett. Sect. **19**, 35–43 (1995).
[3] A. Gruverman, O. Auciello, and H. Tokumoto, Appl. Phys. Lett. **69**, 3191–3193 (1996).
[4] E. L. Colla, S. Hong, D. V. Taylor, A. K. Tagantsev, N. Setter, and K. No, Appl. Phys. Lett. **72**, 2763–2765 (1998).
[5] J. W. Hong, G. H. Noh, S.-I. Park, S. I. Kwun, and Z. G. Khim, Phys. Rev. B **58**, 5078–5084 (1998).
[6] R. S. Muller and T. I. Kamins, *Device Electronics For Integrated Circuits* (Wiley, New York, 1986), p. 31.
[7] C. Kittel, *Introduction to Solid State Physics* (Wiley, Singapore, 1991), p. 61.
[8] R. Luthi and E. Meyer, Phys. Rev. Lett. **76**, 4291–4291 (1996).
[9] G. Zavala, J. H. Fendler, and S. Troiler-McKinstry, J. Appl. Phys. **81**, 7480–7491 (1997).
[10] E. L. Colla, D. V. Taylor, S. Hong, A. K. Tagantsev, K. No, and N. Setter, Integr. Ferroelectr. **22**, 237–244 (1998).
[11] S. Hong, E. L. Colla, E. Kim, D. V. Taylor, A. K. Tagantsev, P. Muralt, K. No, and N. Setter, J. Appl. Phys. **86**, 607–613 (1999).
[12] S. Hong, J. Woo, H. Shin, J.-U. Jeon, Y. E. Pak, K. No, E. L. Colla, and N. Setter (unpublished work).